

## Supporting Information

Subramaniam et al.

### SI Materials and Methods

**Materials.** We purchased manganese (II) chloride tetrahydrate (ACS Reagent Grade), perfluorodecalin (95 % pure), Allura Red AC (dye content 80 %) from Sigma Aldrich. Polystyrene particles were purchased from Invitrogen. Heavy Liquid was purchased from GeoSciences Inc. Polymeric components, such as poly(methyl methacrylate) (PMMA), polytetrafluoroethylene (Teflon) and polyoxymethylene (Delrin), were purchased from McMaster-Carr and custom machined: PMMA sheets with a thickness  $\ell = 6.35$  mm, rods with a diameter  $\ell = 6.35$  mm, tubes with an outer diameter  $\ell = 6.35$  mm and inner diameter of 5.56 mm were cut into rectangular, circular, and annular blocks with different thickness,  $T$ ; Delrin and PMMA sheets were cut into equilateral triangular prisms ( $\ell = 6.67$  mm) with different  $T$ . Polyamide (Nylon 6/6) screws (2 cm in length) were purchased from McMaster-Carr.

**Levitation of Objects in MagLev.** We used commercially available NdFeB magnets — square magnets ( $5.0 \times 5.0 \times 2.5$  cm) or disc magnets (4.8 cm in diameter, 2.5 cm thick), which are capable of providing surface fields of  $\sim 0.4$  T. We levitated objects in an aqueous solution of  $\text{MnCl}_2$  in a rectangular glass container ( $4.5 \times 3.0 \times 4.5$  cm). We adjusted the concentration of  $\text{MnCl}_2$  to yield a solution that had a density that was similar to that of the object so that the object levitated close to the center of the device. We sonicated the solution for one minute to remove air bubbles. After waiting a minimum of three minutes, to allow the object to levitate to

its equilibrium height and orientation, we took an image of the objects in the device, using a Nikon DS-50 digital camera. We measured the orientation angle,  $\alpha$ , from the photographs using ImageJ (NIH Bethesda). We used a digital angle indicator (McMaster-Carr, accuracy of  $0.01^\circ$ ) when rotating the device.

**Fabrication of Armored Droplets.** We spread a monolayer of polystyrene particles onto an air/water interface by adding dropwise a suspension of polystyrene particles in ethanol. The ethanol spread on the water surface and evaporated, thus depositing the particles on the surface. Once a complete monolayer had formed, we added perfluorodecalin dropwise onto the surface of this monolayer. The perfluorodecalin formed a lens-shaped drop and eventually, with additional volume, overcame the surface tension of the water and penetrated the surface of the liquid, and sank. Perfluorodecalin has a density higher than water ( $\rho=1.95 \text{ g/cm}^3$ ). The droplet picked up a jammed monolayer of particles from the water surface. These particles were trapped at the interface of the perfluorodecalin droplet and did not desorb. We produced two coated droplets that we then fused to form the peanut shaped object by squeezing the droplets between two glass plates(12). We then added  $\text{MnCl}_2$  and a commercial water-based density matching liquid (Heavy Liquid,  $\rho=2.85 \text{ g/cm}^3$ , Geoliquids Inc) and levitated the non-spherical droplet in the MagLev device.

## SI Figures

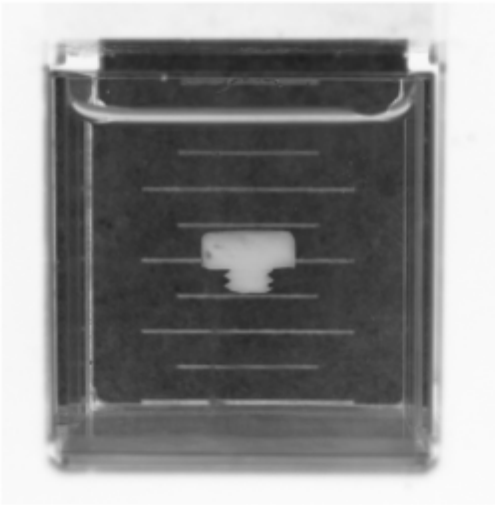


**Fig. S1.** The orientation of objects does not depend on its levitation height in the MagLev device. We imaged the levitating Nylon screw along the  $y$ - $z$ - plane. We progressively increased the density of the paramagnetic medium by adding sucrose, while keeping  $[\text{MnCl}_2]$  constant at 1.0 M. The orientation of the screw did not change with levitation height. The distance between the lines in the ruled scale in the background is 5 mm.

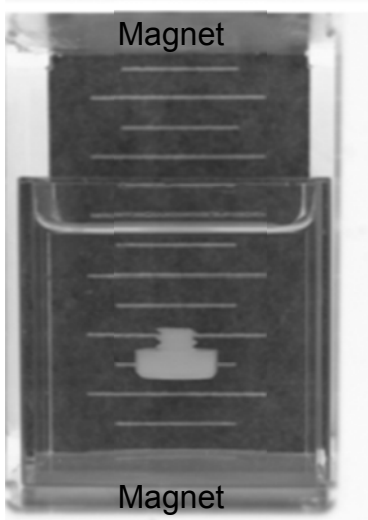
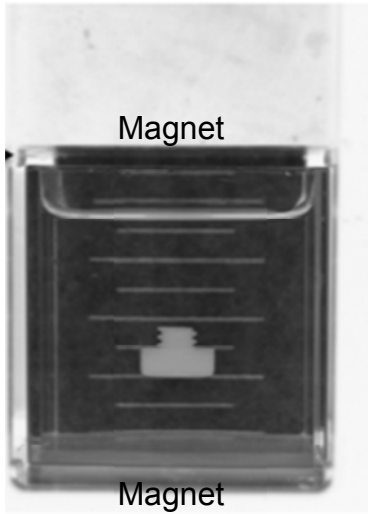


**Fig. S2.** The orientation of objects is insensitive to the separation distance between the magnets. We imaged the levitating Nylon screw along the  $y$ - $z$ - plane. The separation distance between the top and bottom magnets: (from top to bottom) 45 mm, 55 mm, and 65 mm. The screw was levitated in 1.0 M  $\text{MnCl}_2$  solution containing sucrose. The orientation of the screw did not change. The distance between the lines in the ruled scale in the background is 5 mm.



**Fig. S3.** Equilibrium orientation of objects in the  $x'$ - $y'$  plane of the MagLev with square magnets. The top image shows the cross pattern that we used as a guide to the eye, the straight black lines in the pattern were aligned along the diagonals of the magnet. We allowed the hollow PMMA cylinder to equilibrate for 3 minutes before imaging. We then perturbed the cylinder by moving the container out of the device several times. The cylinder orients along the diagonals of the magnet. The behavior of the cylinder is expected based on the location of the minima in the magnetic field in this plane. Scale bar 5 mm.



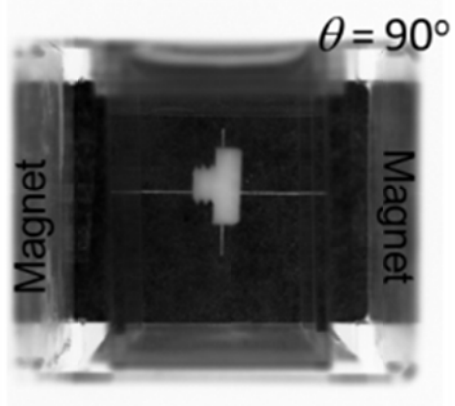
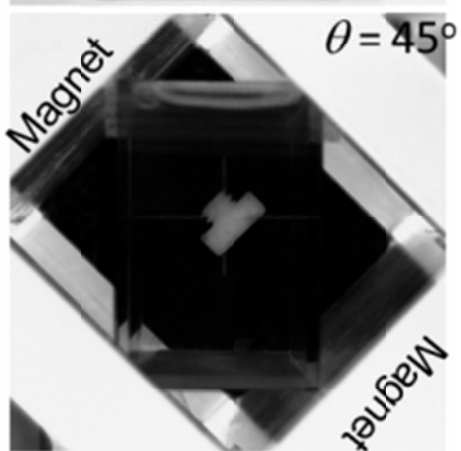
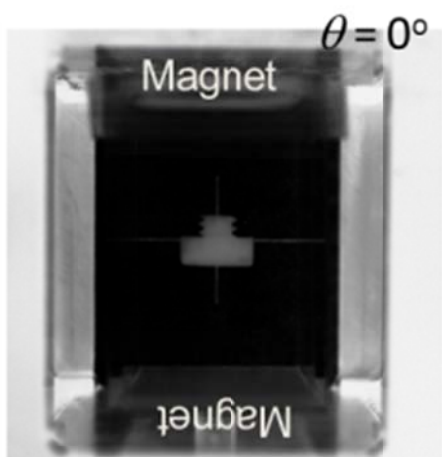


**Fig. S4.** Keeping the container stationary while rotating the device as a means of manipulating the orientation of objects. We placed the container containing the screw and the paramagnetic liquid on a pedestal. We then rotated the MagLev device with respect to the container. The object tracked the position of the magnets. The cross in the background was fixed relative to the laboratory frame of reference. With this configuration, the top of the container remained open and accessible, allowing external grippers, for example, to retrieve the oriented objects. For scale, the horizontal line in the cross is 30 mm.

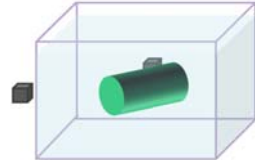
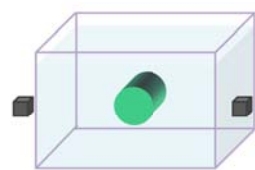
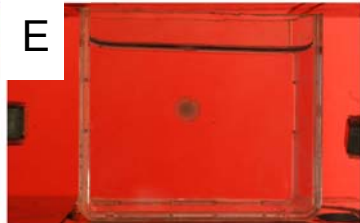
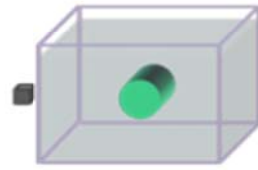
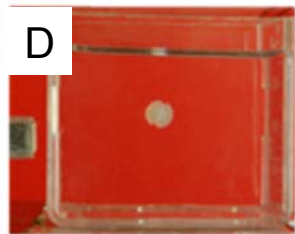
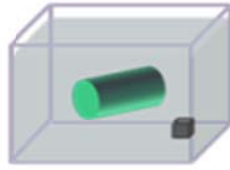
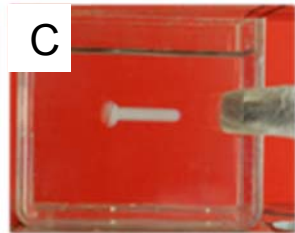
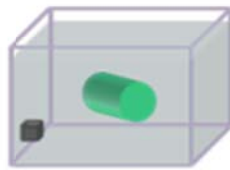
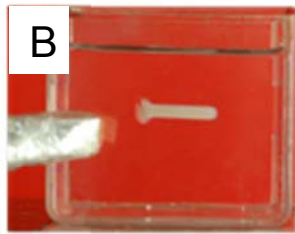
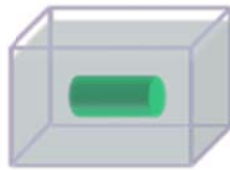
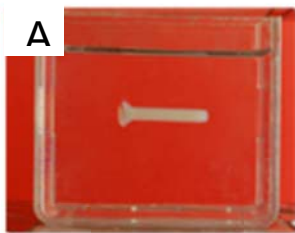
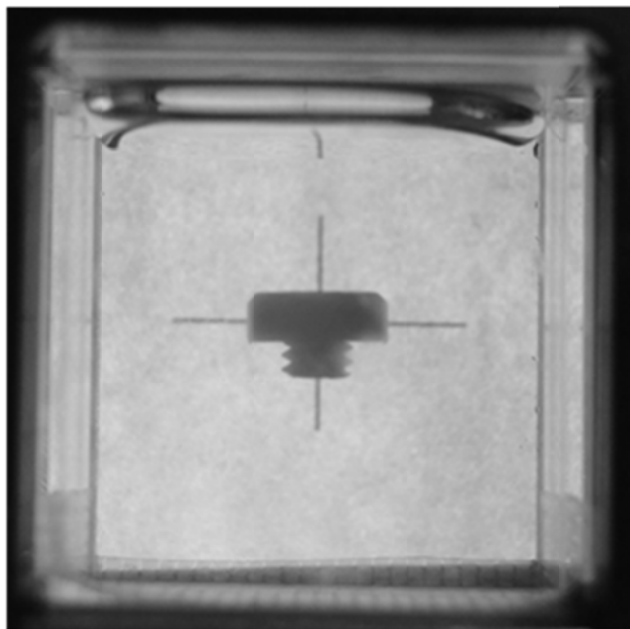


**Fig. S5.** Manipulating the orientation of an object in the  $xy$ - plane with an external magnet. (A) Initial orientation of a Nylon screw (2 cm in length) levitating in the MagLev device. The orientation of the screw was controlled by using (B-D) one or (E-F) two external magnet(s) . The screw remained in its new position orientation after the magnet(s) was/were removed. Schemes on the right show the orientation of the objects.

A



B

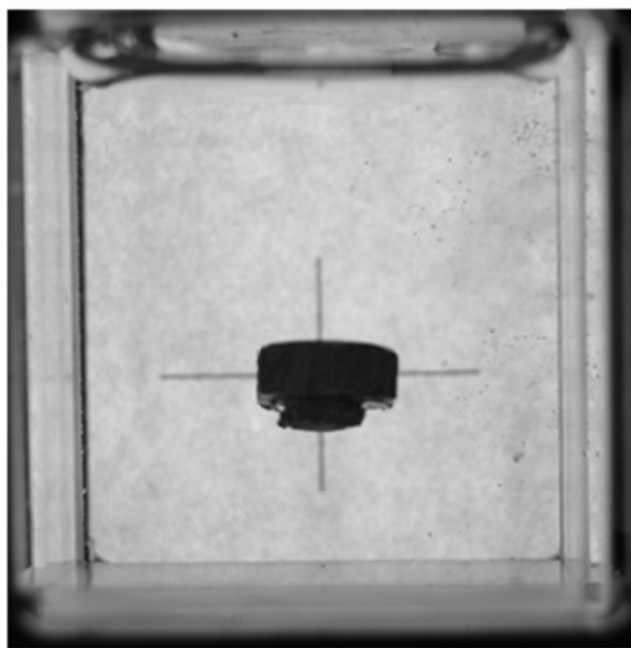


**Fig. S6** Manipulation of objects with metallic or paramagnetic components. (A) A Nylon screw levitating in the MagLev device. The paramagnetic solution is  $[\text{MnCl}_2] = 1.0 \text{ M}$ . (B) The same screw wrapped in aluminum foil and levitating in the device. The orientation of the object did not change.

## SI Text

In our experiments, we observed that objects of homogeneous density and anisotropic shape levitating in a MagLev device moved to a stable levitation height away from the surface of the magnets and adopted a stable orientation with respect to the magnetic field. The orientation of the object depended on the object's shape and its aspect ratio. As the aspect ratio of the object was increased, we observed that the objects changed orientation sharply at a critical aspect ratio.

In the following sections, we present a general theory for the orientation and levitation of arbitrary objects in MagLev. The layout of the SI is as follows. In section I, we obtain an analytical closed form approximation of the magnetic field in a MagLev device. In Section II, we derive the potential energy of an arbitrary object in a MagLev device and find expressions for the equilibrium height and equilibrium orientation of the object. We conclude: (i) the levitation height of the centroid of an object depends only on its average density and its average susceptibility. The levitation height does not depend on the the distribution of these quantities within an object. This result greatly simplifies calculations for objects of heterogeneous density and/or magnetic susceptibility; (ii) a homogeneous object has only two potential stable configurations in the MagLev. The configuration that is preferred (i.e. of lowest potential energy) depends only on the ratio of second moments of area of the object. This result is consistent with a torque balance, but is more general and proves that the levitating object does not have any metastable orientations. In section III, we calculate the potential energy of the levitating objects used in experiments and obtain analytical predictions for the critical aspect ratio,  $A_R$  at which transitions in orientation occur. The theoretical values are in excellent agreement with experiments.

# 1 Expression for the Magnetic Field in the Magnetic Levitation Device

We assume that the MagLev device is stationary with respect to the laboratory frame of reference. Thus the fixed coordinates (i.e., the laboratory frame of reference), the  $x$ -,  $y$ -,  $z$ -axes, as defined in the main text, is always coincident with the body-fixed  $x'$ -,  $y'$ -,  $z'$ - axes of the MagLev device. To simplify the notation, we equate these two coordinates and define the “MagLev frame of reference” as  $\vec{r} = (x, y, z)$ .

The Maglev device consists of two coaxial circular or square magnets with like poles facing set a distance  $d$  apart. We choose the  $z$  axis (unit vector  $\mathbf{e}_z$ ) to be the axis of symmetry and define the upper surface of the bottom magnet to be  $z = 0$  and the lower surface of the top magnet to be at  $z = d$ . This simple configuration between the two magnets sets up a rather complicated magnetic field that is a function of axial and radial positions.

In our experiments we find that the orientation of the object in the plane perpendicular to the surface of the magnets is independent of the shape of the magnets. Thus, to simplify the analysis, we consider the radially symmetric case, and let the lateral extent of the magnetic field to be  $R$ . The axial symmetry allows the expression of the magnetic field in the volume between the magnets  $-R \leq x \leq R$ ,  $-R \leq y \leq R$  and  $0 \leq z \leq d$ , in cylindrical coordinates, approximately as a field that is a function of  $z$  and  $\rho = \sqrt{x^2 + y^2}$ ,  $\mathbf{B}(\rho, z)$ . Note that the term  $\rho$  used in this section is different from the use of  $\rho$  for the mass density. For  $\rho$  used to refer to mass density we always have a subscript to refer to the object.

We next obtain an approximation for the field,  $\mathbf{B}(x, y, z)$ , between two magnets in the absence of the paramagnetic medium. Solving Maxwell’s equations yields the magnetic field - this is however complicated to attempt analytically. The field generated by two-loops of wire of radius  $R$  through which a current  $I$  flows, arranged in the



anti-Helmholtz configuration yields to leading order:

$$B_z = 3I\mu_o \left(\frac{d}{2}R^2\right) \left[\left(\frac{d}{2}\right)^2 + R^2\right]^{-\frac{5}{2}} \left(z + \frac{d}{2}\right) + \dots \quad (1)$$

$$B_\rho = -\frac{3}{2}I\mu_o \left(\frac{d}{2}R^2\right) \left[\left(\frac{d}{2}\right)^2 + R^2\right]^{-\frac{5}{2}} \rho + \dots \quad (2)$$

Here,  $\mu_o$  is the permeability of free space. The region of field minimum is at the center of the device equidistant from the surface of the magnets. The field is maximum at the surface of the magnets, i.e. at  $z = 0$  and  $d$ , and the magnitude of  $B_o$  can, in principle, be a function of  $z$  and  $\rho$ . A single permanent magnet can be modeled as an infinite number of loops extending from  $R = 0$  to  $R = R_m$ , where  $R_m$  is the radius of the magnet. Thus, integrating, and keeping only leading order terms, the field due to permanent magnets in the anti-Helmholtz configuration is expected to have the form

$B_z \approx \left[\int_0^{R_m} 3I\mu \left(\frac{d}{2}R^2\right) \left[\left(\frac{d}{2}\right)^2 + R^2\right]^{-\frac{5}{2}} dR\right] \left(z + \frac{d}{2}\right)$  which on rearranging yields approximate expressions

$$B_z = B_{o,z} \left(1 - 2\frac{z}{d}\right), \quad \text{and} \quad (3)$$

$$B_\rho = B_{o,\rho} \left(\frac{\rho}{R}\right) \quad (4)$$

Thus, the field is approximately

$$\mathbf{B}^o(x, y, z) \approx B_{o,z} \left(1 - 2\frac{z}{d}\right) \mathbf{e}_z + \frac{1}{\sqrt{2}}B_{o,\rho} \left(\frac{\rho}{R}\right) \mathbf{e}_x + \frac{1}{\sqrt{2}}B_{o,\rho} \left(\frac{\rho}{R}\right) \mathbf{e}_y. \quad (5)$$

The magnetic flux lines are perpendicular close to the surface of the magnets but curve appreciably at the center. Thus, although the magnetic field is zero at the point equidistant between the magnets, this is also a point of inflexion of the flux lines. When a paramagnetic liquid, of magnetic susceptibility  $\chi_m$ , is introduced between the magnets, the magnetic field will change. To leading order, one may approximate the field by the linear

term in  $z$  - this is the Taylor series expansion about the point  $\rho = 0$  where only the term due to the geometric symmetries of the two-magnet configuration is retained. Thus (consistent with Mirica et. al. (2)) we write approximately

$$\mathbf{B}(x, y, z) \approx B_o \left(1 - 2\frac{z}{d}\right) \mathbf{e}_z. \quad (6)$$

For a linear variation in  $z$ ,  $B_o$  is constant.

## 2 Equilibrium Orientation and Position of an Object of Arbitrary Shape in a Linearly Varying Magnetic Field

### 2.1 Total Energy

Consider a dielectric object, of volume  $V$ , in an paramagnetic medium suspended in a uniform magnetic field defined in (6). The object has a magnetic susceptibility  $\chi_o(\vec{r})$  and density  $\rho_o(\vec{r})$ . These quantities may vary as a function of position, parametrized by the vector  $\vec{r} = (x, y, z)$ , within the object. The magnetic susceptibility of the medium is  $\chi_m$ . To simplify calculations, we take advantage of the symmetry of the magnetic field and define the origin,  $O$ , of the MagLev frame of reference at  $z + d/2$ . Therefore  $z$  is measured relative to the center of the device (where  $B = 0$ ) and  $\mathbf{B} = \frac{2B_o}{d}z\mathbf{e}_z$ . Since both  $\chi(\vec{r})_o \ll 1$  and  $\chi_m \ll 1$ , the warping of the field is negligible; the object does not significantly modify the shape of the magnetic field lines. This assumption is true for most diamagnetic objects and paramagnetic media. Equation (7) gives the potential energy density due to the magnetic field within the volume of the object.

$$\begin{aligned}
u_{mag} &= -\frac{1}{2} \frac{\Delta\chi(\vec{r})}{\mu_0} \mathbf{B} \cdot \mathbf{B} = -\frac{\Delta\chi(\vec{r})}{2\mu_0} \left( \frac{2B_s}{d} z \right)^2 = -\frac{2\Delta\chi(\vec{r})B_0^2}{\mu_0 d^2} z^2 \\
&= \beta \Delta\chi(\vec{r}) z^2
\end{aligned} \tag{7}$$

In this equation,  $\Delta\chi(\vec{r}) = \chi_o(\vec{r}) - \chi_m$ , and we have defined the constant  $\beta = -\frac{2B_0^2}{\mu_0 d^2}$ . Equation (8) gives the potential energy density due to the gravitational field within the volume of the object.

$$u_{grav} = \Delta\rho(\vec{r})gz, \tag{8}$$

Integrating the energy density over the volume of the object provides the potential energy of the system. (Equations (9) and (10)).

$$U_{mag} = \int_V u_{mag} dV = \beta \int_V \Delta\chi(\vec{r}) z^2 dV \tag{9}$$

$$U_{grav} = \int_V u_{grav} dV = g \int_V \rho(\vec{r}) z dV \tag{10}$$

In these equations,  $dV$  is the volume element in the MagLev frame of reference. The total energy of the MagLev system is  $U = U_{mag} + U_{grav}$ .

We next define a body-fixed frame of reference for the object, with origin  $O'$ . Translation and rotation of the object within the MagLev frame of reference can be described relative to this “object frame of reference”. The object frame of reference is chosen arbitrarily (at first). We will provide in the subsequent sections a method to find the ideal reference frame that simplifies calculations.

Within this object frame of reference, we define  $\vec{r}' = (x', y', z')$  to be the coordinates. Since the magnetic field in our approximation only varies in  $z$ , we take the origin  $O'$  to be along the  $z'$  axis. Any rotation of the object frame of reference in the MagLev frame of

reference can be described as a rotation by an angle  $\alpha$  around some axis defined by  $\mathbf{e}_u = (\sin \theta \cos \phi, \sin \theta \sin \phi, \cos \theta)$ . We use spherical coordinates to describe the MagLev frame of reference:  $\theta$  is the declination angle from  $z$ , and  $\phi$  is the azimuthal angle measured from  $x$ . The axis of rotation will always lie in the  $xy$ -plane such that  $\theta = \pi/2$  and  $\mathbf{e}_z = (\cos \phi, \sin \phi, 0)$ . A rotation by an angle  $\alpha$  about the unit vector  $\mathbf{e}_u$  can be represented by the rotation matrix in Equation (11).

$$A = \begin{pmatrix} \cos \alpha + (1 - \cos \alpha) \cos^2 \phi & (1 - \cos \alpha) \cos \phi \sin \phi & \sin \alpha \sin \phi \\ (1 - \cos \alpha) \cos \phi \sin \phi & \cos \alpha + (1 - \cos \alpha) \sin^2 \phi & -\cos \phi \sin \alpha \\ -\sin \alpha \sin \phi & \cos \phi \sin \alpha & \cos \alpha \end{pmatrix} \quad (11)$$

Any configuration of the object in the MagLev can be treated as a pure rotation by  $A$  of the original arbitrarily chosen configuration (which may not correspond to the minimal energy configuration of the object) plus a vertical translation  $\vec{h} = (0, 0, h)$ . The coordinate transformation from the object frame of reference to the MagLev frame of reference is given by Equation (12).

$$\vec{r} = A\vec{r}' + \vec{h}. \quad (12)$$

Since the energy only depends on  $z$ , we need only to find  $z = \mathbf{e}_z \cdot \vec{r}$ , which reduces to Equation (13).

$$\begin{aligned} z &= \mathbf{e}_z \cdot (A\vec{r}' + \vec{h}) = (\mathbf{e}_z A) \vec{r}' + \mathbf{e}_z \cdot \vec{h} \\ &= \begin{pmatrix} -\sin \alpha \sin \phi \\ \sin \alpha \cos \phi \\ \cos \alpha \end{pmatrix} \cdot \begin{pmatrix} x' \\ y' \\ z' \end{pmatrix} + h \\ &= -x' \sin \alpha \sin \phi + y' \sin \alpha \cos \phi + z' \cos \alpha + h \end{aligned} \quad (13)$$

Using Equation (13) we re-write the magnetic and gravitational potential energies in the object frame of reference.

$$U_{mag} = \beta \int_{V'} \Delta\chi(\vec{r}) (-x' \sin \alpha \sin \phi + y' \sin \alpha \cos \phi + z' \cos \alpha + h)^2 dV' \quad (14)$$

$$U_{grav} = g \int_{V'} \Delta\rho(\vec{r}') (-x' \sin \alpha \sin \phi + y' \sin \alpha \cos \phi + z' \cos \alpha + h) dV'. \quad (15)$$

The behavior of  $U$  will depend on the zeroth, first, and second moments of the functions  $\Delta\chi(\vec{r})$  and  $\Delta\rho(\vec{r}')$  defined on the volume  $V'$  of the object. Expansion of these integrals will result in many terms. Choosing an appropriate object frame of reference (we call this frame of reference the “principal frame of reference”) however, will result in many terms vanishing. We now proceed to describe a procedure for finding the principal frame of reference.

## 2.2 Moments of a Function

Consider an arbitrary object with volume  $V$  defined in an object frame of reference  $O'$  with body-fixed coordinates  $\vec{r}' = (x', y', z')$ . We define a general scalar function  $f(x', y', z')$  inside the object, and  $f = 0$  everywhere outside the object (Fig. 1). The moments of this general function  $f(x', y', z')$  is given by Equation (16).

$$M_f^{ijk} = \int_{V'} x'^i y'^j z'^k f(x', y', z') dV'. \quad (16)$$

The center of  $f$ , in Cartesian coordinates, which we define as  $(\bar{x}'_f, \bar{y}'_f, \bar{z}'_f)$  is given by

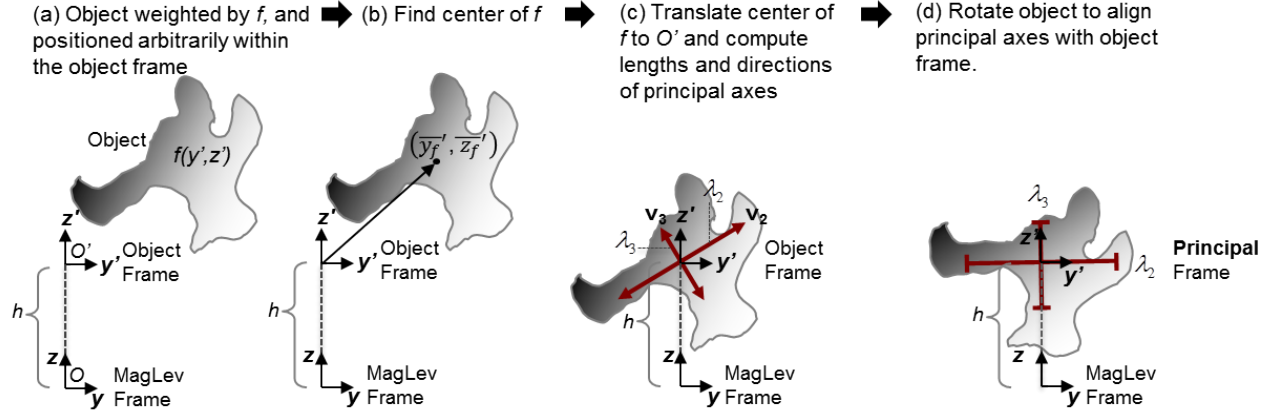


Figure S7: Procedure for finding the principal frame of reference of an arbitrarily oriented object in the MagLev. For clarity, we only show a 2D cross section of the object. Analyzing the orientational potential energy in the principal frame simplifies calculations.

Equations (17-19).

$$\bar{x}'_f = \frac{\int_V x' f(x', y', z') dV'}{\int_V f(x', y', z') dV'} = \frac{M_f^{100}}{M_f^{000}} \quad (17)$$

$$\bar{y}'_f = \frac{\int_V y' f(x', y', z') dV'}{\int_V f(x', y', z') dV'} = \frac{M_f^{010}}{M_f^{000}} \quad (18)$$

$$\bar{z}'_f = \frac{\int_V z' f(x', y', z') dV'}{\int_V f(x', y', z') dV'} = \frac{M_f^{001}}{M_f^{000}} \quad (19)$$

For example, if  $f = \text{const}$ , then  $M_0^{000} = V'$  and  $(\bar{x}', \bar{y}', \bar{z}')$  is the geometric centroid of the object. If  $f = \chi(x', y', z')$ , then  $M_\chi^{000} = \int \chi(x', y', z') dV' = \bar{\chi} V'$ , and  $(\bar{x}'_\chi, \bar{y}'_\chi, \bar{z}'_\chi)$  is the center of susceptibility. If  $f = \rho(x', y', z')$ , then  $M_\rho^{000} = \bar{\rho} V'$ , and  $(\bar{x}'_\rho, \bar{y}'_\rho, \bar{z}'_\rho)$  is the center of mass.

To find the principal axes and orientation of the object, we define the second order central moments of the object  $\mu_f^{ijk}$  (Equation (20)).

$$\mu_f^{ijk} = \frac{M_f^{ijk}}{M_f^{000}} - \bar{x}'_f^i \bar{y}'_f^j \bar{z}'_f^k \quad (20)$$

We construct the covariance matrix of the function  $f$  (Equation (21)).

$$cov[f(x', y', z')] = \begin{bmatrix} \mu_f^{200} & \mu_f^{110} & \mu_f^{101} \\ \mu_f^{110} & \mu_f^{020} & \mu_f^{011} \\ \mu_f^{101} & \mu_f^{011} & \mu_f^{002} \end{bmatrix} \quad (21)$$

The covariance matrix allows calculation of the length and direction of the three principal axes of the object. The eigenvectors ( $\mathbf{v}_1, \mathbf{v}_2, \mathbf{v}_3$ ) of the covariance matrix correspond to the principal axes of the object, weighted by the function  $f(x', y', z')$ . The eigenvalues ( $\lambda_1^2, \lambda_2^2, \lambda_3^2$ ) correspond to the squared length of the three principal axes. By constructing a rotation matrix  $Q = [\mathbf{v}_1 \mathbf{v}_2 \mathbf{v}_3]$  composed of the eigenvectors, we can perform a change of coordinates  $\bar{\mathbf{r}}' \rightarrow Q\bar{\mathbf{r}}'$  that will rotate the object such that its principal axes are parallel to the axes of the MagLev frame of reference.

If we translate  $(\bar{x}'_f, \bar{y}'_f, \bar{z}'_f)$  to  $O'$ , then  $\bar{x}'_f = \bar{y}'_f = \bar{z}'_f = 0$ , and  $M_f^{100} = M_f^{010} = M_f^{001} = 0$ . If we also rotate the object frame of reference by applying  $Q$ , then  $\mathbf{v}_1$  will be aligned with the x-axis. In this principal frame of reference, the covariance matrix is diagonalized, i.e. the axes of the object will be collinear with the axes of the MagLev frame of reference. Therefore,  $\mu_f^{110} = \mu_f^{101} = \mu_f^{011} = 0$  and  $M_f^{110} = M_f^{101} = M_f^{011} = 0$ . In this principal frame of reference, the integrals of all first order terms and second order cross-terms vanish, and the lengths of the principal axes reduces to Equations (22-24).

$$\lambda_1^2 = \frac{M_f^{200}}{M_f^{000}} = \frac{\int_{V'} x'^2 f(x', y', z') dV'}{\int_{V'} f(x', y', z') dV'} \quad (22)$$

$$\lambda_2^2 = \frac{M_f^{020}}{M_f^{000}} = \frac{\int_{V'} y'^2 f(x', y', z') dV'}{\int_{V'} f(x', y', z') dV'}. \quad (23)$$

$$\lambda_3^2 = \frac{M_f^{002}}{M_f^{000}} = \frac{\int_{V'} z'^2 f(x', y', z') dV'}{\int_{V'} f(x', y', z') dV'}. \quad (24)$$

## 2.3 Magnetic Potential Energy

We can simplify  $U_{mag}$  by applying the above steps to an object, i.e. by orienting the object in its principal frame of reference, and then by inspecting each of the nine terms separately.

$$\begin{aligned}
U_{mag}^{200} &= \beta \sin^2 \alpha \sin^2 \phi \int_{V'} x'^2 \Delta \chi(\vec{r}') dV' = \beta \sin^2 \alpha \sin^2 \phi M_\chi^{200} \\
&= \beta \Delta \bar{\chi} V \lambda_1^2 \sin^2 \alpha \sin^2 \phi
\end{aligned} \tag{25}$$

$$\begin{aligned}
U_{mag}^{020} &= \beta \sin^2 \alpha \cos^2 \phi \int_{V'} y'^2 \Delta \chi(\vec{r}') dV' = \beta \sin^2 \alpha \cos^2 \phi M_\chi^{020} \\
&= \beta \Delta \bar{\chi} V \lambda_2^2 \sin^2 \alpha \cos^2 \phi
\end{aligned} \tag{26}$$

$$\begin{aligned}
U_{mag}^{002} &= \beta \cos^2 \alpha \int_{V'} z'^2 \Delta \chi(\vec{r}') dV' = \beta \sin^2 \alpha M_\chi^{002} \\
&= \beta \Delta \bar{\chi} V \lambda_3^2 \cos^2 \alpha
\end{aligned} \tag{27}$$

$$U_{mag}^{110} \propto \int_{V'} x' y' \Delta \chi(\vec{r}') dV' = M_\chi^{110} = 0 \tag{28}$$

$$U_{mag}^{101} \propto \int_{V'} x' z' \Delta \chi(\vec{r}') dV' = M_\chi^{101} = 0 \tag{29}$$

$$U_{mag}^{011} \propto \int_{V'} y' z' \Delta \chi(\vec{r}') dV' = M_\chi^{011} = 0 \tag{30}$$

$$U_{mag}^{100} \propto \int_{V'} x' \Delta \chi(\vec{r}') dV' = M_\chi^{100} \propto \bar{x}_\chi = 0 \tag{31}$$

$$U_{mag}^{010} \propto \int_{V'} y' \Delta \chi(\vec{r}') dV' = M_\chi^{010} \propto \bar{y}_\chi = 0 \tag{32}$$

$$U_{mag}^{001} \propto \int_{V'} z' \Delta \chi(\vec{r}') dV' = M_\chi^{001} \propto \bar{z}_\chi = 0 \tag{33}$$

$$U_{mag}^{000} = \beta h^2 \int_{V'} \Delta \chi(\vec{r}') dV' = \beta h^2 \Delta \bar{\chi} V, \tag{34}$$

To obtain the preceding equations, we used the relations defined by equations (22), (23), and (24) along with  $M_\chi^{000} = \Delta \bar{\chi} V$ . The total magnetic potential energy  $U_{mag} = \sum_{ijk} U_{mag}^{ijk}$  is therefore given by Equation (35).

$$\begin{aligned}
U_{mag} &= U_{mag}^{200} + U_{mag}^{020} + U_{mag}^{002} + U_{mag}^{000} \\
&= \beta \Delta \bar{\chi} V (\lambda_1^2 \sin^2 \alpha \sin^2 \phi + \lambda_2^2 \sin^2 \alpha \cos^2 \phi + \lambda_3^2 \cos^2 \alpha + h^2) \\
&= \beta \Delta \bar{\chi} V [\lambda_2^2 - \lambda_3^2 + (\lambda_1^2 - \lambda_2^2) \sin^2 \phi] \sin^2 \alpha + \beta \Delta \bar{\chi} V h^2,
\end{aligned} \tag{35}$$



To obtain Equation (35), we dropped terms that are constant with respect to the two degrees of freedom,  $\alpha$  and  $h$ . We define ratios of the second moment of susceptibility  $R_y$  (Equation (36)) and  $R_z$  (Equation (37)) of the object.

$$R_y = \left( \frac{\lambda_2}{\lambda_1} \right)^2 \quad (36)$$

$$R_z = \left( \frac{\lambda_3}{\lambda_1} \right)^2, \quad (37)$$

such that

$$U_{mag} = \beta \Delta \bar{\chi} V \lambda_1^2 [R_y - R_z + (1 - R_y) \sin^2 \phi] \sin^2 \alpha + \beta \Delta \bar{\chi} V h^2. \quad (38)$$

This result is the full three-dimensional form of the magnetic potential energy for an arbitrary object that is parametrized within a MagLev (laboratory) frame of reference.

The angle  $\alpha$  is the angle of declination of the  $z'$ -axis from the  $z$ -axis. The angle  $\phi$  defines the axis within the  $xy$ -plane about which the object rotates. If we did not use the principal frame of reference construction, Equations (28-33) would be non-zero and the calculations would be more complex.

## 2.4 Gravitational Potential Energy

Using a similar procedure, we expand the gravitational potential energy into four terms.

$$\begin{aligned} U_{grav}^{(100)} &= -g \sin \alpha \sin \phi \int_{V'} x' \Delta \rho(\vec{r}') dV' = -g \sin \alpha \sin \phi M_\rho^{100} \\ &= -mg \bar{x}'_\rho \sin \alpha \sin \phi \end{aligned} \quad (39)$$

$$\begin{aligned} U_{grav}^{(010)} &= g \sin \alpha \cos \phi \int_{V'} y' \Delta \rho(\vec{r}') dV' = g \sin \alpha \cos \phi M_\rho^{010} \\ &= mg \bar{y}'_\rho \sin \alpha \cos \phi \end{aligned} \quad (40)$$

$$\begin{aligned} U_{grav}^{(001)} &= g \cos \alpha \int_{V'} z' \Delta \rho(\vec{r}') dV' = g \cos \alpha M_\rho^{001} \\ &= mg \bar{z}'_\rho \cos \alpha \end{aligned} \quad (41)$$

$$\begin{aligned} U_{grav}^{(000)} &= gh \int_{V'} \Delta \rho(\vec{r}') dV' = gh M_\rho^{000} \\ &= mgh, \end{aligned} \quad (42)$$

In this equation,  $\vec{r}'_\rho = (\bar{x}'_\rho, \bar{y}'_\rho, \bar{z}'_\rho)$  is the position of the center of mass of the principal frame of reference. Equation (43) gives the total gravitational energy of the object.

$$\begin{aligned} U_{grav} &= mg (h - \bar{x}'_\rho \sin \alpha \sin \phi + \bar{y}'_\rho \sin \alpha \cos \phi + \bar{z}'_\rho \cos \alpha) \\ &= mg (h - \vec{r}'_\rho \cdot \mathbf{e}'_z), \end{aligned} \quad (43)$$

In this equation,  $\mathbf{e}'_z = e_z A = (\sin \alpha \sin \phi, \sin \alpha \cos \phi, \cos \alpha)$ , which is the z-axis unit vector parametrized in the object frame of reference. Thus, the gravitational potential energy depends only the height of the object  $h$  and the z- component of the center of mass, as expected.

## 2.5 Equilibrium Height

The magnitude of the gravitational field is constant everywhere in the MagLev device, whereas the magnitude of the magnetic field depends on position. Thus, we expect the levitation height of the center of the object will not depend on the specific distribution of density within the object. It will only depend on the mean density of the object. The equilibrium height  $h_0$  occurs where  $\frac{\partial U}{\partial h} = 0$ .

$$\frac{\partial U}{\partial h} = \frac{\partial U_{mag}}{\partial h} + \frac{\partial U_{grav}}{\partial h} = 2\beta\Delta\bar{\chi}Vh_0 + \Delta\bar{\rho}Vg = 0, \quad (44)$$

Equation (45) gives the equilibrium levitation height of an arbitrary object in the MagLev.

$$h_0 = -\frac{g\Delta\bar{\rho}}{2\beta\Delta\bar{\chi}}. \quad (45)$$

Expanding the constants we obtain Equation (46).

$$h_0 = \frac{(\bar{\rho}_o - \rho_m)g\mu_0 d^2}{(\bar{\chi}_o - \chi_m)4B_0^2} \quad (46)$$

This result proves that the levitation height of an object in a MagLev device (relative to the center of susceptibility of the object) *does not depend on the specific local distribution of susceptibility (and density) within the object*. The levitation height of the center of susceptibility of the object (which may differ from the centroid) is wholly determined by its mean density and mean susceptibility.

If the susceptibility (and/or the density) is distributed homogeneously (or with specific symmetries) within the object, then the center of susceptibility (and/or the center of mass) corresponds to the geometric centroid of the object. If we define  $h$  relative to the face of the bottom magnet, we obtain Equation (47).

$$h_0 = \frac{(\rho_o - \rho_m)g\mu_0 d^2}{(\chi_o - \chi_m)4B_0^2} + \frac{d}{2}, \quad (47)$$

This equation is consistent with equation 5 of Mirica *et. al.* (2).

We conclude that the position and orientation of the objects are decoupled, provided that the magnetic field is linear. Therefore, in a linear magnetic field, we can minimize with respect to the height to find the equilibrium position, and then minimize independently with respect to orientation to calculate the equilibrium orientation of an object. The decoupling allows the use of coordinate transformations such as those in Section 2.2 and 2.3 (which simplify calculations by making many terms zero), to perform calculations independent of the actual equilibrium levitation height of the object in the device.

## 2.6 Potential Energy of Orientation for a Homogenous Object

For objects of homogenous susceptibility and density, we can make the following simplifications: (i)  $\Delta\chi(\vec{r}) = \Delta\chi$  and  $\Delta\rho(\vec{r}) = \Delta\rho$ ; (ii)  $\vec{r}_\rho = 0$  and there is no gravitational torque ( $\frac{\partial U_{grav}}{\partial \alpha} = 0$ ); (iii)  $\lambda_1^2$ ,  $\lambda_2^2$ , and  $\lambda_3^2$  reduce to the second moments of area of the object. All the objects that we tested experimentally had a pair of degenerate second moments (a square prism, a cylinder, a hollow cylinder, and an equilateral prism). The second moment of area,  $R_y$  is 1, if we orient our principal frame of reference so that the first two principal axes are degenerate ( $\lambda_1 = \lambda_2$ ). We thus can define a single parameter,  $R$  that is a ratio of second moments that characterizes fully the behavior of objects with double degenerate geometries (Equation (48)).

$$R = \frac{R_z}{R_y} = \left( \frac{\lambda_z}{\lambda_y} \right)^2. \quad (48)$$

Equation (49) gives the total potential energy for objects with double degenerate geometries.

$$U = \beta V \Delta\chi \lambda_1^2 (R_y - R_z) \sin^2 \alpha + \beta V \Delta\chi h^2 + \Delta\rho V g h. \quad (49)$$

To calculate the orientation of an object, we consider only the angle dependent part

$U(\alpha)$  of the potential energy, which is given by Equation (50).

$$\begin{aligned} U(\alpha) &= \beta V \Delta \chi \lambda_2^2 (1 - R) \sin^2 \alpha \\ &\propto (1 - R) \sin^2 \alpha. \end{aligned} \tag{50}$$

The equilibrium orientations occur at the local minima of  $U(\alpha)$ . The extrema of this function occur at  $\alpha = 0, \pi/2, \pi$ , and  $3\pi/2$  (the function is periodic). The sign of  $(1 - R)$  determines which of these are minima and which are maxima. If  $R < 1$ , then  $U(\alpha) \propto \sin^2 \alpha$  and the minima occur at  $\alpha = 0$  and  $\alpha = \pi$ . If  $R > 1$ , then  $U(\alpha) \propto -\sin^2 \alpha \propto \cos^2 \alpha$  and the minima occur at  $\alpha = \pi/2$  and  $\alpha = 3\pi/2$ . If  $R = 1$ , then  $U(\alpha) = 0$  and the potential energy is degenerate; the object does not have any preferred orientation. For this system, the orientation is completely determined by the value of  $R$ ; the major axis (largest eigenvalue) of the sample will always align perpendicular to the magnetic gradient (z-axis). Intuitively, the magnetic field acts to both displace the object away from the magnets (levitation), and orient in a way such that the object appears to be “as small as possible” relative to the magnetic gradient.

## 2.7 The Effect of Non-Linearities of the Magnetic Field on the Orientation of Dimensionally Degenerate Objects of Homogeneous Density

We have analyzed the effects of non-linearities in the magnetic field on degenerate shapes to show that the non-linear terms qualify the energy minima. The full analysis is lengthy, thus we outline the basic steps here. First, as mentioned in the previous section, the magnetic field plateaus when approaching the surface of the magnets and has an inflexion point at the center. Therefore, the non-linearity of the field can be approximated by  $\mathbf{B} = B_0 z + B_1 z^3 + O(z^5)$  where  $B_0$  is the linear coefficient of the magnetic field and  $B_1$  is

the cubic coefficient of the magnetic field. The contribution of the cubic term cancels part of the linear term, since the magnetic field stops increasing in magnitude as fast when away from the center.

Assuming that the higher order terms are small compared to the leading one, the magnetic energy density is then given by Equation (51).

$$u_{mag} \approx \frac{\Delta\chi}{2\mu_0} B_0^2 z^2 + \frac{\Delta\chi}{2\mu_0} 2B_0 B_1 z^4 = c_1 z^2 + c_2 z^4. \quad (51)$$

In this equation,  $c_1 = \frac{\Delta\chi}{2\mu_0} B_0^2$  and  $c_2 = \frac{\Delta\chi}{2\mu_0} 2B_0 B_1$  and ( $c_1 > 0, |c_2| \ll c_1$ ).

Here,  $c_2 > 0$  if  $B_1$  and  $B_0$  have the same sign, and  $c_2 < 0$  if  $B_1$  and  $B_0$  have different signs.

Equation (52) gives the total magnetic potential energy.

$$U_{mag} = \int_V u_{mag} = \int_{V_0} (c_1 z^2 + c_2 z^4) dV = U_1 + U_2, \quad (52)$$

In this equation,  $V_0$  is the shape of the object,  $U_1 = c_1 \int_{V_0} z^2 dV$ , and  $U_2 = c_2 \int_{V_0} z^4 dV$ .

At equilibrium, this energy is again minimized as the system is conservative with no dissipation. We analyze an object oriented in its principal frame of reference and, without loss of generality, consider a 2D cross-section in the  $yz$ -plane. Since  $U_1 \gg U_2$  for small objects, the behavior of a non-degenerate case ( $R < 0$  or  $R > 0$ ) is dominated by  $U_1$ , as expected, for which there are no metastable states. For the dimensionally degenerate case ( $R=1$ ), such as for a square, the energy  $U_1 = 0$ . Within this 2D cross-section,  $z = y' \sin \alpha + z' \cos \alpha$ , and following a procedure similar to that in the previous section we

find that for  $U_2 = \sum_{ij} U_2^{ij}$ :

$$U_2^{4,0} = c_2 \sin^4 \alpha \int_{V_0} y'^4 dV \quad (53)$$

$$U_2^{3,1} = 4c_2 \cos \alpha \sin^3 \alpha \int_{V_0} y'^3 z'^1 dV \quad (54)$$

$$U_2^{2,2} = 6c_2 \cos^2 \alpha \sin^2 \alpha \int_{V_0} y'^2 z'^2 dV \quad (55)$$

$$U_2^{1,3} = 4c_2 \cos^3 \alpha \sin^1 \alpha \int_{V_0} y'^1 z'^3 dV \quad (56)$$

$$U_2^{0,4} = c_2 \cos \alpha^4 \int_{V_0} z'^4 dV, \quad (57)$$

which rely on the fourth geometric moments of the shape. For a square with side length  $\ell$ ,  $U_2^{3,1} = U_2^{1,3} = 0$  the remaining potential energy is:

$$\begin{aligned} U_2 &= c_2 \frac{\ell^6}{480} (\cos(4\alpha) - 7) \\ &\propto \cos(4\alpha) \end{aligned} \quad (58)$$

For a superlinear magnetic field ( $c_2 > 0$ ) (the field increases with an exponent greater than 1), Equation (58) shows that there are four stable configurations:  $\alpha = 0^\circ, 90^\circ, 180^\circ, 270^\circ$ . For a sublinear magnetic field ( $c_2 < 0$ ), there are also four stable configurations:  $\alpha = 45^\circ, 135^\circ, 225^\circ, 315^\circ$ . Based on our experimental observations of the orientation of the objects, it appears that the field is slightly superlinear in our typical MagLev setup. Simulations of the magnetic field using Mathematica, also demonstrates that the field is superlinear in the vertical direction (results not shown).

### 3 Specific Calculations for Objects in the Experiments

In the previous sections, we demonstrated analytically how principles of symmetry in conjunction with a simplified linear form for the magnetic field provides predictions for the orientation of objects in the MagLev. Due to the minimization of magnetic potential energy, homogeneous objects can orient only along their principal axis of symmetry in a linear magnetic field. To compare theory to experiments, in this section, we present specific calculations for the objects used in our experiments. The experimental objects have a pair of degenerate principle axes ( $\lambda_1 = \lambda_2$ ). We choose a body-fixed principal reference frame such that one of the degenerate axes ( $\lambda_1$ ) remains collinear with the  $x$ - and  $x'$ -axes. In this reference frame, all rotation is constrained to the  $yz$ -plane (around the  $x$ - and  $x'$ -axes). We can, therefore, use Equation (50) to analyze the change in potential energy due to the orientation of the object. We define a unit vector  $\mathbf{p}$  perpendicular to the face that spans the degenerate principal axes, and measure the angle  $\alpha$  as the angle of inclination between  $\mathbf{p}$  and the  $z$ -axis (Fig. 2 in the main paper and Fig. S8). We prepare the object in an initial state  $\alpha = 0$  (configuration 1). We expect that an object will abruptly transition from  $\alpha = 0$  to  $\alpha = 90^\circ$  (configuration 2) when its second moment ratio  $R$  transitions from  $R < 1$  to  $R > 1$ .  $R$  can be calculated using Equation (59).

$$R = \left( \frac{\lambda_3}{\lambda_2} \right)^2 = \frac{\int_V z^2 dV}{\int_V y^2 dV} \quad (59)$$

Although  $R$  is a parameter that wholly predicts the orientation of a homogeneous object in a linear field, this value cannot, typically, be easily measured experimentally. We parametrize our objects with a pair of length parameters,  $\ell$  for the characteristic width of the face of the object, and  $T$  for the thickness (Fig. S8). Here we calculate  $R$  for various shapes and relate it to the easily measured aspect ratio,  $A_R = T/\ell$ . In the experiments,



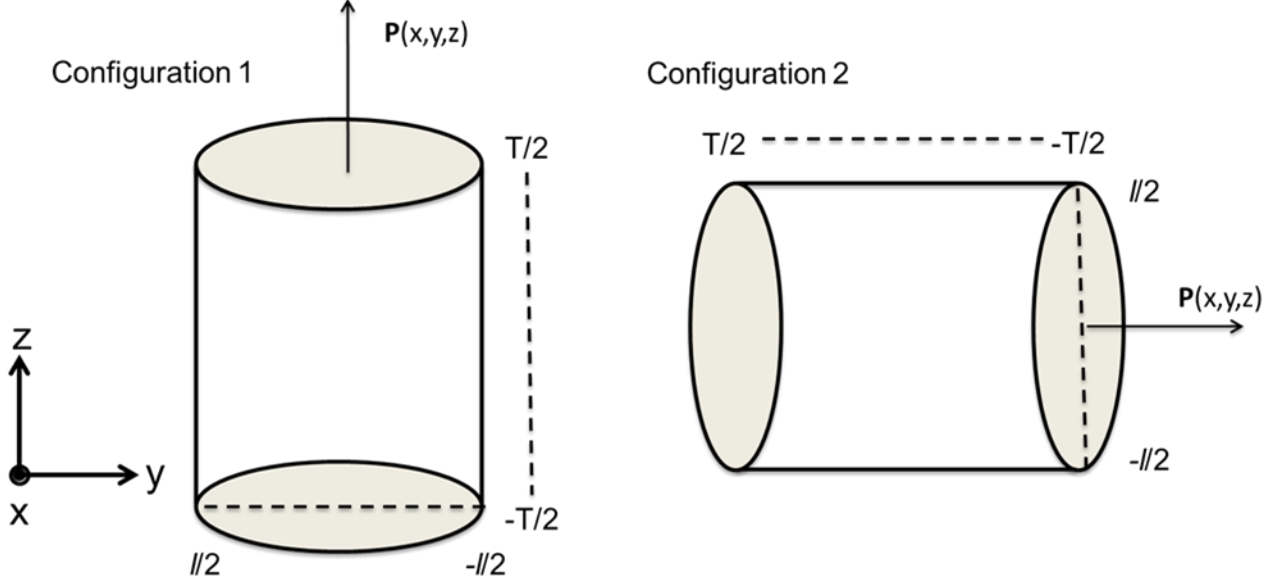


Figure S8: Sketch of the configuration of a cylinder with the bounds of integration marked.

one dimension ( $\ell$ ) was kept constant while the other ( $T$ ) was varied so as to change  $A_R$  (and therefore  $R$ ).

### 3.1 Solid block of cross section area $\ell \times \ell$ and length $T$

For a solid rectangular block, we use Cartesian coordinates for integration.

$$R = \frac{\int_{V_0} z^2 dV}{\int_{V_0} y^2 dV} = \frac{\int_{-T/2}^{T/2} z^2 dz \int_{-\ell/2}^{\ell/2} dy \int_{-\ell/2}^{\ell/2} dx}{\int_{-T/2}^{T/2} dz \int_{-\ell/2}^{\ell/2} y^2 dy \int_{-\ell/2}^{\ell/2} dx} = \frac{l^2 T^3 / 12}{\ell^4 T / 12} = \frac{T^2}{\ell^2} = A_R^2, \quad (60)$$

and therefore

$$A_R = \sqrt{R}. \quad (61)$$

The critical aspect ratio is therefore  $A_R = 1$ , matching experiment. For  $A_R < 1$ , the object will orient in configuration 1.

### 3.2 Solid cylinder of diameter $\ell$ and height $T$

For a solid cylinder, we use cylindrical coordinates to simplify integration.

$$R = \frac{\int_{V_0} z^2 dV}{\int_{V_0} y^2 dV} = \frac{\int_{-T/2}^{T/2} z^2 dz \int_0^{2\pi} d\phi \int_0^{\ell/2} r dr}{\int_{-T/2}^{T/2} dz \int_0^{2\pi} \int_0^{\ell/2} (r \sin \phi)^2 r dr d\phi} = \frac{\frac{\pi}{48} \ell^2 T^3}{\frac{\pi}{64} \ell^4 T} = \frac{4T^2}{3\ell^2} = \frac{4}{3} A_R^2, \quad (62)$$

and therefore

$$A_R = \sqrt{\frac{3}{4}} R. \quad (63)$$

The critical aspect ratio is therefore  $A_R = \sqrt{3/4} \approx 0.86$ , matching experiment. For  $A_R < 0.86$ , the object will orient in configuration 1.

### 3.3 Hollow cylinder of outer diameter $\ell$ , inner diameter $\epsilon\ell$ and length $T$

For a hollow cylinder, we continue use cylindrical coordinates to simplify integration.

$$R = \frac{\int_{V_0} z^2 dV}{\int_{V_0} y^2 dV} = \frac{\int_{-T/2}^{T/2} z^2 dz \int_0^{2\pi} d\phi \int_{\epsilon\ell/2}^{\ell/2} r dr}{\int_{-T/2}^{T/2} dz \int_0^{2\pi} \int_{\epsilon\ell/2}^{\ell/2} (r \sin \phi)^2 r dr d\phi} = \frac{\frac{\pi}{48} \ell^2 T^3 (1 - \epsilon^2)}{\frac{\pi}{64} \ell^4 T (1 - \epsilon^4)} \quad (64)$$

$$= \frac{4(1 - \epsilon^2)T^2}{3(1 - \epsilon^4)\ell^2} = \frac{4(1 - \epsilon^2)}{3(1 - \epsilon^4)} A_R^2, \quad (65)$$

and therefore

$$A_R = \sqrt{\frac{3(1 - \epsilon^4)}{4(1 - \epsilon^2)}} R. \quad (66)$$

We note that increasing  $\epsilon$  (making a hollow cylinder) will increase the critical aspect ratio for the change in orientation - indeed we get critical aspect ratios that are greater than unity for a range of  $\epsilon$ . When  $\epsilon = 0$ , we recover the result for a solid cylinder. When  $\epsilon = 1$ , there is no cylinder. For a range of  $\epsilon$ , we have critical aspect ratios of greater than unity. For the experiments the outer diameter of the hollow cylinder is 1/4 inch and the thickness

of the wall is  $1/32$  inch (i.e.  $\epsilon = 3/4$ ). Substituting these values, we find the critical aspect ratio to be  $A_R \approx 1.09$  matching experiment. For  $A_R < 1.09$ , the object will orient in configuration 1.

### 3.4 Triangular block

For a triangular block, we use Cartesian coordinates to parametrize the limits of integration.

$$R = \frac{\int_{V_0} z^2 dV}{\int_{V_0} y^2 dV} = \frac{\int_{-T/2}^{T/2} z^2 dz \int_{-l/2}^{l/2} dx \int_{-\ell/2\sqrt{3}}^{-\sqrt{3}|x|+\ell/\sqrt{3}} dy}{\int_{-T/2}^{T/2} dz \int_{-l/2}^{l/2} dx \int_{-\ell/2\sqrt{3}}^{-\sqrt{3}|x|+\ell/\sqrt{3}} y^2 dy} = \frac{\frac{1}{16\sqrt{3}}\ell^2 T^3}{\frac{1}{32\sqrt{3}}\ell^4 T} \quad (67)$$

$$= 2\frac{T^2}{\ell^2} = 2A_R^2, \quad (68)$$

and therefore

$$A_R = \sqrt{\frac{R}{2}}. \quad (69)$$

The critical aspect ratio is therefore  $A_R = \sqrt{1/2} \approx 0.70$ , matching experiment. For  $A_R < 0.7$ , the object will orient in configuration 1.

## Supporting Information References

1. Jackson JD (1998) *Classical Electrodynamics* (John Wiley Sons, New York) 3 Ed.

2. Mirica KA, Shevkoplyas SS, Phillips ST, Gupta M, Whitesides GM (2009)

Measuring densities of solids and liquids using magnetic levitation: Fundamentals. *J. Am. Chem. Soc.* 131(29):10049-10058.